Int. J. Heat Mass Transfer. Vol. 35, No. 2, pp. 559–565, 1992
Printed in Great Britain

0017-9310/92 \$5.00+0.00

Step response of the crossflow heat exchanger with finite wall capacitance

MARCO SPIGA
Istituto di Fisica Tecnica, Università di Bologna, Viale Risorgimento 2, 40136 Bologna, Italy

and

GIAMPIERO SPIGA
Dipartimento di Matematica, Università di Bari, Via Fortunato, 70125 Bari, Italy

(*Received* 31 *October* 1990)

Abstract—The step response of a single-pass crossflow heat exchanger is investigated. The two-dimensional transient temperature distributions in the core wall and in both the unmixed fluids are analytically determined, considering finite wall heat capacity (i.e. finite propagation speed of disturbances). The solutions are deduced by the local energy balance equations, resorting to the Green functions and to a threefold Laplace transform. The dimensionless temperatures are presented in terms of the governing parameters (number of transfer units, capacity ratios, heat transfer resistance ratio). Assuming constant initial conditions and entrance temperature of the hot fluid subjected to a sudden step increase, the transient temperature field is computed with extremely low computational time; the results are plotted for a wide range of the governing parameters.

INTRODUCTION

MORE DETAILED and accurate investigations about the knowledge of the transient fluid temperature distribution inside heat exchangers are required nowadays, to provide correct evaluation of thermal and structural performances. Recently, problems related to crossflow heat exchangers have increased their relevance in several advanced industrial applications (gas turbine regenerators, air–sodium units in nuclear engineering, ceramic exchangers, chemical engineering, food processing, cryogenics). Any variation in the working conditions, either intentional or accidental, produces a perturbation which propagates all over the heat exchanger, with important consequences for control devices of fluid regulation. The time lag associated with the fluid response to perturbation can be an interesting parameter for performance considerations and safety requirements.

In the last few years many authors have focused their interest on searching for analytical solutions of the crossflow heat exchanger problem. While the steady-state solution is now well established [1], only recently the general transient problem has been tackled with analytical methods. In the past some authors obtained numerical [2] or analytical solutions [3], but were restricted to simplified hypotheses such as large wall capacitance (i.e. infinite velocity of propagation of any disturbance) and determination of the mixed mean exit temperatures only. A more general analytical solution, dealing with different kinds of perturbation, is given, but still for large wall capacitance, in refs. [4, 5], where a more exhaustive discussion about previous literature can be found. Only very recently an improved solution for the complete mathematical model, taking account of the finite wall heat capacity, has been worked out in ref. [6], but solutions are presented only for a delta-like pulse.

This paper is aimed at reporting on the exact analytical solution for the transient two-dimensional temperature distributions in crossflow heat exchangers, following a step change in the inlet temperature of the hot fluid. The availability of these analytical solutions can reduce the need of scale model testing (sometimes prohibitively expensive) and constitutes an accurate benchmark for the validation of computer codes. The solutions are expressed as integrals of the Green functions, and involve modified Bessel functions. The influence of the governing physical parameters is appropriately commented on.

ASSUMPTIONS AND FUNDAMENTAL EQUATIONS

The theoretical analysis is based on the classical assumptions adopted for the description of direct transfer, single-pass crossflow heat exchangers, with walls separating the two fluid streams (flowing at right angles). The investigation is carried out according to the following hypotheses:

(a) both fluids are unmixed (as well known, the assumption of one fluid mixed introduces a strong simplification of the problem);

(b) all the physical properties and the fluid capacity rates are constant;

(c) the exchanger shell or shroud is adiabatic;

(d) the mass velocities at the entrance of the heat exchanger on each side are constant and change of flow distribution is neglected;

NOMENCLATURE

A	heat transfer surface [m^2]
c	specific heat at constant pressure [J kg^{-1} K^{-1}]
E	flow capacitance ratio
$G(.)$	Green function
h	heat transfer coefficient [W m^{-2} K^{-1}]
$I(.)$	modified Bessel function of the first kind
L	exchanger length [m]
$\mathscr{L}$	Laplace operator
m	mass flow rate [kg s^{-1}]
M	mass of the exchanger [kg]
N	dimensionless exchanger length
NTU	number of transfer units
R	heat transfer resistance ratio
s, p, q	Laplace transform variables
t	dimensionless time variable
T	dimensionless temperature
u	fluid velocity [m s^{-1}]
$U(.)$	Heaviside step function
V	heat capacity ratio
x, y	dimensionless space variables.

Greek symbols

γ	incomplete gamma function
$\delta(.)$	Dirac delta function
Θ	temperature [K]
Θ_0	initial temperature of the whole unit [K]
$\Delta\Theta$	step increase in the inlet temperature of the hot fluid [K]
ξ, η	space variables [m]
τ	time variable [s]
φ	primary fluid inlet temperature [K].

Subscripts

a	primary (hot) fluid
b	secondary (cold) fluid
i	general label
w	solid wall.

(e) axial heat conduction is negligible;

(f) the geometrical configuration is constant throughout the exchanger;

(g) the inlet temperature of the unstepped fluid is constant and equal to the initial temperature of the whole unit;

(h) the thermal conductances on both sides are constant and inclusive of wall thermal resistance and fouling.

This last hypothesis implies that the wall temperatures are the same on both sides, even if the thermal conductivity of the exchanger core is finite. However, the heat transfer balance between the fluids is fulfilled, since the fluid–wall thermal conductances are appropriately reduced to account for the core thermal resistance and the fouling factor.

The five dimensionless physical parameters typical of steady-state heat transfer phenomena in heat exchangers are

$$E = (mc)_b/(mc)_a, \qquad R = (hA)_b/(hA)_a,$$
$$N_i = (hA)_i/(mc)_i \qquad i = \mathrm{a, b}$$
$$NTU = \{(mc)_{\min}[1/(hA)_a + 1/(hA)_b]\}^{-1}. \quad (1)$$

Of course only two of them are independent since

$$RN_a = EN_b$$
$$N_a = E\,NTU(1+R)/R \quad \text{and} \quad N_b = (1+R)NTU \qquad \text{if } E \leqslant 1$$
$$N_a = NTU(1+R)/R \quad \text{and} \quad N_b = NTU(1+R)/E \qquad \text{if } E > 1.$$

For transient phenomena two more parameters take on a fundamental relevance, since they are associated to the finite propagation speed of disturbances, namely

$$V_i = L_i(mc)_i/Mc_w u_i \qquad i = \mathrm{a, b}. \quad (2)$$

Moreover, it is suitable to introduce the following dimensionless variables:

$$x = \xi(hA)_a/(mc)_a L_a, \qquad y = \eta(hA)_b/(mc)_b L_b$$
$$t = \tau(hA)_a/Mc_w, \qquad T_i = (\Theta_i - \Theta_0)/\Delta\Theta \qquad i = \mathrm{a, b, w} \quad (3)$$

where the constant $\Delta\Theta$ is some typical or averaged value of $\Theta_a(0, y, t) - \Theta_0$. The governing differential equations, expressing conservation of energy in a control volume for wall and fluids, are

$$\frac{\partial T_w}{\partial t} + (1+R)T_w = T_a + RT_b$$
$$\frac{\partial T_a}{\partial x} + V_a\frac{\partial T_a}{\partial t} + T_a = T_w$$
$$\frac{\partial T_b}{\partial y} + \frac{V_b}{R}\frac{\partial T_b}{\partial t} + T_b = T_w \quad (4)$$

for $t > 0$, $0 < x < N_a$, $0 < y < N_b$. Having in mind here only perturbations induced by a sudden variation of the primary fluid inlet temperature, the initial and boundary conditions upon which equations (4) must be solved will be prescribed as

$$T_i(x, y, 0) = 0 \qquad i = \mathrm{a, b, w}$$
$$T_a(0, y, t) = \varphi(y, t)$$
$$T_b(x, 0, t) = 0. \quad (5)$$

The step response (in which $\Theta_a(0, y, t) - \Theta_0$ is actually a constant) is easily reproduced by setting $\varphi(y,t) = 1$. The temperature fields obtained in this latter important case will simulate the sudden startup of the exchanger, and the transient regime taking place before the steady-state operating conditions are reached.

ANALYTICAL SOLUTION

The linearity of the problem allows the introduction of the Green's functions $G_i(x,y,t)$, solving the same set of differential equations, equation (4), as the sought temperatures $T_i(x,y,t)$, but with initial boundary conditions

$$\begin{aligned} &G_i(x,y,0) = 0 \qquad i = \mathrm{a,b,w} \\ &G_\mathrm{a}(0,y,t) = \delta(y)\delta(t) \\ &G_\mathrm{b}(x,0,t) = 0. \end{aligned} \tag{6}$$

The Green's functions G_i provide the solution for the temperature fields induced by any inlet datum by means of the convolution integrals

$$T_i(x,y,t) = \int_0^y \mathrm{d}y' \int_0^t G_i(x,y',t')\varphi(y-y',t-t')\,\mathrm{d}t'. \tag{7}$$

Taking a threefold Laplace transform with respect to t, x, y with complex parameters s, p, q, respectively, and defining

$$\begin{aligned} G_i'''(p,q,s) &= \mathscr{L}_p\mathscr{L}_q\mathscr{L}_s[G_i(x,y,t)] \\ &= \int_0^\infty \exp(-st)\,\mathrm{d}t \int_0^\infty \exp(-px)\,\mathrm{d}x \\ &\quad \times \int_0^\infty \exp(-qy) G_i(x,y,t)\,\mathrm{d}y \end{aligned} \tag{8}$$

leads to the set of algebraic equations for G_i'''

$$\begin{cases} (s+R+1)G_\mathrm{w}'''(p,q,s) - G_\mathrm{a}'''(p,q,s) - RG_\mathrm{b}'''(p,q,s) = 0 \\ (p+V_\mathrm{a}s+1)G_\mathrm{a}'''(p,q,s) - G_\mathrm{w}'''(p,q,s) = 1 \\ (q+1+V_\mathrm{b}s/R)G_\mathrm{b}'''(p,q,s) - G_\mathrm{w}'''(p,q,s) = 0 \end{cases} \tag{9}$$

whose solution is

$$\begin{cases} G_\mathrm{w}'''(p,q,s) = (q+1+V_\mathrm{b}s/R)G_\mathrm{b}'''(p,q,s) \\ G_\mathrm{a}'''(p,q,s) = [(s+R+1)(q+1+V_\mathrm{b}s/R) \\ \quad -R]G_\mathrm{b}'''(p,q,s) \\ G_\mathrm{b}'''(p,q,s) = [(s+R+1)(p+V_\mathrm{a}s+1) \\ \quad \times(q+1+V_\mathrm{b}s/R) - (q+1+V_\mathrm{b}s/R) \\ \quad -R(p+V_\mathrm{a}s+1)]^{-1}. \end{cases} \tag{10}$$

The problem is thus reduced to a threefold Laplace inversion of equations (10). The first inverse transform with respect to p is simply a matter of residue calculation and yields

$$\begin{aligned} G_\mathrm{b}''(x,q,s) &= (s+r+1)^{-1}\left(q+\frac{V_\mathrm{b}}{R}s+1-\frac{R}{s+R+1}\right) \\ &\quad \times \exp\left[-x\left(V_\mathrm{a}s+1-\frac{1}{s+R+1}\right)\right. \\ &\quad \left. + x\frac{R}{(s+R+1)^2}\left(q+\frac{V_\mathrm{b}}{R}s+1-\frac{R}{s+R+1}\right)^{-1}\right]. \end{aligned} \tag{11}$$

Further inversion with respect to the variables q and s require the formulae [7]

$$\begin{aligned} &\mathscr{L}_y^{-1}[\exp(k/q)/q] = I_0[2(ky)^{1/2}] \\ &\mathscr{L}_t^{-1}\left\{\frac{1}{s}\exp[(k+h)/s]I_0[2(kh)^{1/2}/s]\right\} \\ &\qquad = I_0[2(kt)^{1/2}]I_0[2(ht)^{1/2}] \end{aligned} \tag{12}$$

and some standard properties of the $\mathscr{L}$ operator. One obtains, after a little algebra

$$\begin{aligned} G_\mathrm{b}(x,y,t) &= U(t-V_\mathrm{a}x-V_\mathrm{b}y/R)\exp[-x-y \\ &\quad -(1+R)(t-V_\mathrm{a}x-V_\mathrm{b}y/R)] \\ &\quad I_0[2x^{1/2}(t-V_\mathrm{a}x-V_\mathrm{b}y/R)^{1/2}]I_0[2R^{1/2}y^{1/2}(t-V_\mathrm{a}x \\ &\quad -V_\mathrm{b}y/R)^{1/2}] \end{aligned} \tag{13a}$$

where the unit step function U takes the finite propagation speed of disturbances in the exchanger into account. Analogous steps are in order for $i = \mathrm{a,w}$; the final results are

$$\begin{aligned} G_\mathrm{a}(x,y,t) &= \exp(-x)\delta(y)\delta(t-V_\mathrm{a}x) + U(t-V_\mathrm{a}x) \\ &\quad \times \exp[-x-(1+R)(t-V_\mathrm{a}x)]\left(\frac{x}{t-V_\mathrm{a}x}\right)^{1/2} \\ &\quad \times I_1[2x^{1/2}(t-V_\mathrm{a}x)^{1/2}]\delta(y) + U(t-V_\mathrm{a}x \\ &\quad -V_\mathrm{b}y/R)(Rx/y)^{1/2}\exp[-x-y-(1+R)(t-V_\mathrm{a}x \\ &\quad -V_\mathrm{b}y/R)]I_1[2x^{1/2}(t-V_\mathrm{a}x-V_\mathrm{b}y/R)^{1/2}]I_1[2R^{1/2}y^{1/2} \\ &\quad \times(t-V_\mathrm{a}x-V_\mathrm{b}y/R)^{1/2}] \end{aligned} \tag{13b}$$

$$\begin{aligned} G_\mathrm{w}(x,y,t) &= U(t-V_\mathrm{a}x)\exp[-x-(1+R)(t-V_\mathrm{a}x)] \\ &\quad \times I_0[2x^{1/2}(t-V_\mathrm{a}x)^{1/2}]\delta(y) + U(t-V_\mathrm{a}x \\ &\quad -V_\mathrm{b}y/R)(R/y)^{1/2}(t-V_\mathrm{a}x-V_\mathrm{b}y/R)^{1/2}\exp[-x-y \\ &\quad -(1+R)(t-V_\mathrm{a}x-V_\mathrm{b}y/R)]I_0[2x^{1/2}(t-V_\mathrm{a}x \\ &\quad -V_\mathrm{b}y/R)^{1/2}]I_1[2R^{1/2}y^{1/2}(t-V_\mathrm{a}x-V_\mathrm{b}y/R)^{1/2}]. \end{aligned} \tag{13c}$$

The solution to the general problem is now given by equations (7) and (13). The step response is easily obtained by putting $\varphi = 1$ in equation (7), and becomes explicitly, for the hot fluid

$$T_\mathrm{a}(x,y,t) = \exp(-x)U(t-V_\mathrm{a}x)\left\{1 + \int_{V_\mathrm{a}x}^{t} \exp[-(1+R)(t'-V_\mathrm{a}x)]\left(\frac{x}{t'-V_\mathrm{a}x}\right)^{1/2} I_1[2x^{1/2}\right.$$

$$\times\,(t'-V_a x)^{1/2}]\,\mathrm{d}t' + (Rx)^{1/2}\int_{V_a x}^{t} \exp[-(1+R)$$

$$\times\,(t'-V_a x)]\,\mathrm{d}t' \int_0^{y^*} \exp\{-[1-V_b(1+R)/R]\,y'\}$$

$$\times\, y'^{-1/2} I_1[2x^{1/2}(t'-V_a x - V_b y'/R)^{1/2}]\, I_1[2R^{1/2} y'^{1/2}$$

$$\left.\times\,(t'-V_a x - V_b y'/R)^{1/2}]\,\mathrm{d}y'\right\} \tag{14a}$$

for the cold fluid

$$T_b(x,y,t) = \exp(-x)\,U(t-V_a x)\int_{V_a x}^{t} \exp[-(1+R)$$

$$\times\,(t'-V_a x)]\,\mathrm{d}t' \int_0^{y^*} \exp\{-[1-V_b(1+R)/R]\,y'\}$$

$$\times\, I_0[2x^{1/2}(t'-V_a x - V_b y'/R)^{1/2}]\, I_0[2R^{1/2} y'^{1/2}$$

$$\times\,(t'-V_a x - V_b y'/R)^{1/2}]\,\mathrm{d}y' \tag{14b}$$

and for the core wall

$$T_w(x,y,t) = \exp(-x)\,U(t-V_a x)$$

$$\times\left\{\int_{V_a x}^{t} \exp[-(1+R)(t'-V_a x)]\, I_0[2x^{1/2}(t'-V_a x)^{1/2}]\,\mathrm{d}t'\right.$$

$$+\int_{V_a x}^{t} \exp[-(1+R)(t'-V_a x)]\,\mathrm{d}t' \int_0^{y^*} \exp\{-[1$$

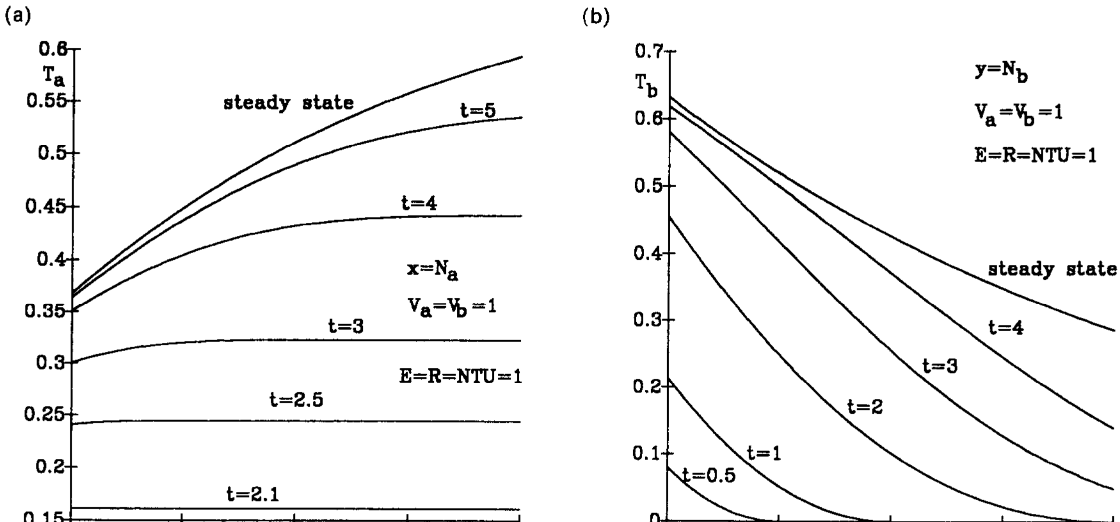

FIG. 1. Fluid temperatures at the outlet sections vs space variable for different values of time when $E = R = NTU = 1$, $V_a = V_b = 1$.

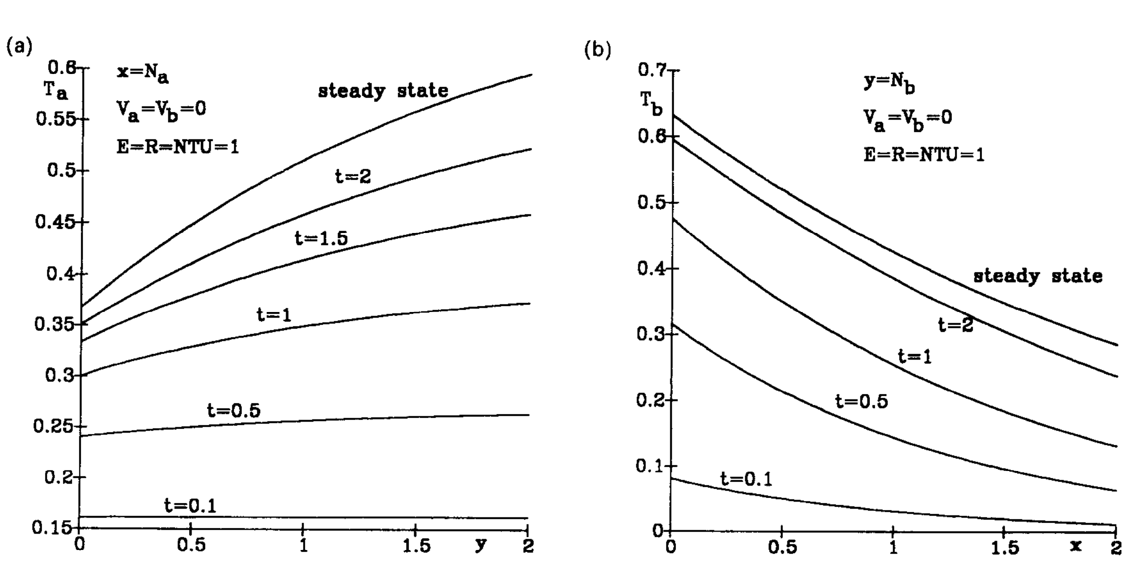

FIG. 2. Fluid temperatures at the outlet sections vs space variable for different values of time when $E = R = NTU = 1$, $V_a = V_b = 0$.

$$
\begin{aligned}
&- V_b(1+R)/R]\,y'\}\left[\frac{R(t'-V_a x)-V_b y'}{y'}\right]^{1/2} \\
&\times I_0[2x^{1/2}(t'-V_a x-V_b y'/R)^{1/2}]\,I_1[2R^{1/2}y'^{1/2} \\
&\times (t'-V_a x-V_b y'/R)^{1/2}]\,\mathrm{d}y'\Big\} \qquad (14c)
\end{aligned}
$$

where

$$y^* = \min\,[y, R(t'-V_a x)/V_b]. \qquad (15)$$

Equation (14) constitutes the exact analytical solution in terms of integrals of modified Bessel functions. The meaning of y^* in connection with propagations in the y-direction at a speed R/V_b has been discussed already in ref. [6]. Propagation in the x-direction at a speed of $1/V_a$ is apparent from equations (14) themselves, where temperatures depend on time only via the combination $t-V_a x$. The double integration required by the explicit solutions (14) does not present technical problems because the integrands are bounded continuous functions of all variables.

RESULTS

The numerical results have been obtained on a Toshiba 3100e personal computer, working in double

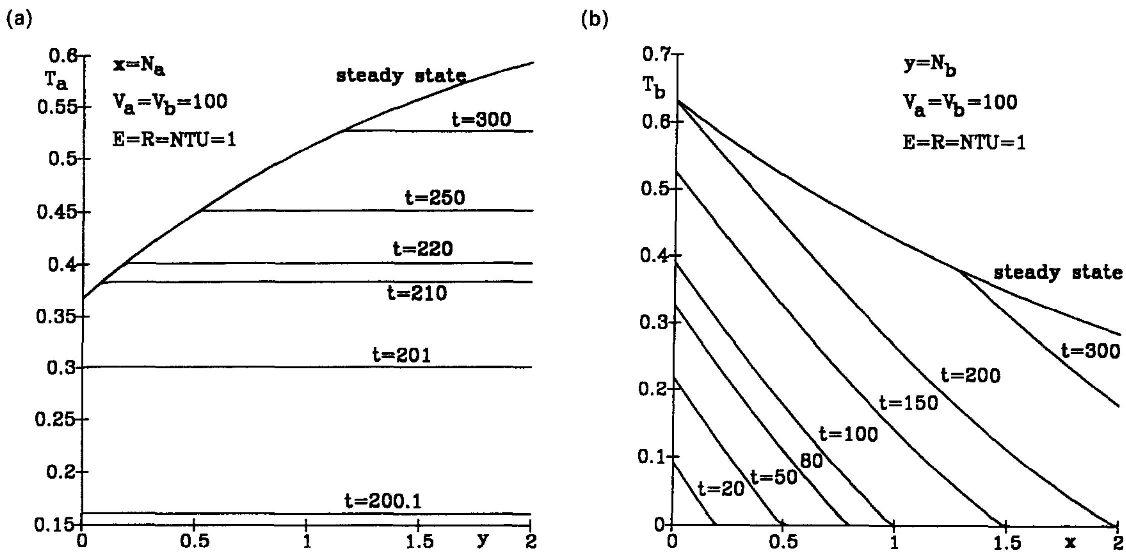

FIG. 3. Fluid temperatures at the outlet sections vs space variable for different values of time when $E = R = NTU = 1$, $V_a = V_b = 100$.

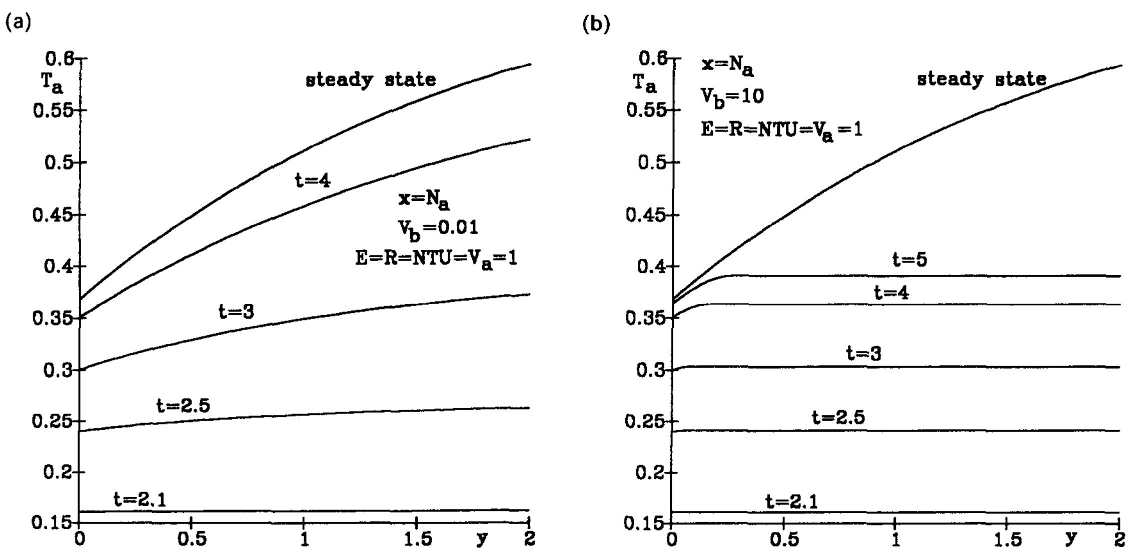

FIG. 4. T_a at $x = N_a$ vs y for different values of time when $E = R = NTU = V_a = 1$: (a) $V_b = 0.01$; (b) $V_b = 10$.

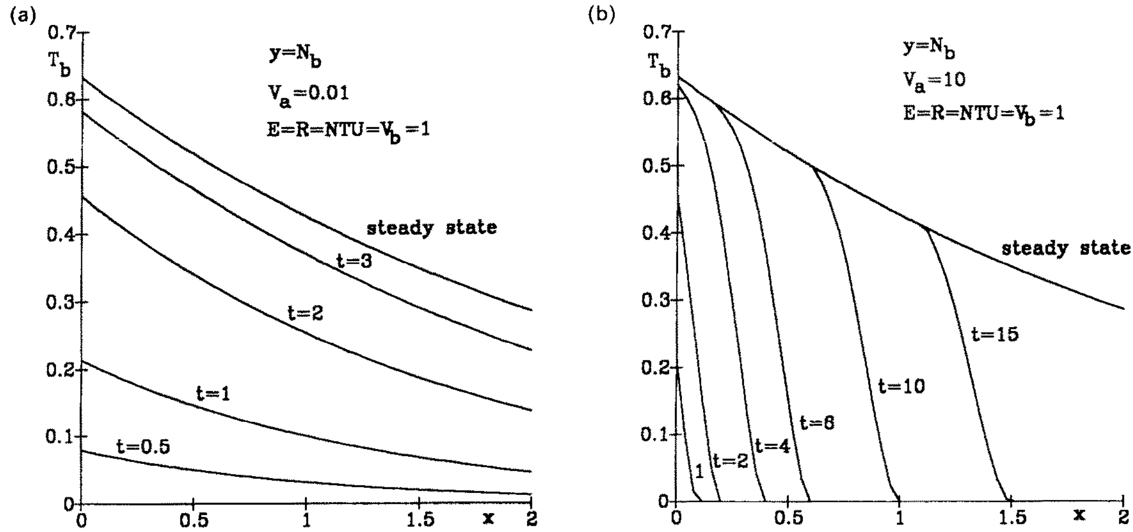

Fig. 5. T_b at $y = N_b$ vs x for different values of time when $E = R = NTU = V_b = 1$: (a) $V_a = 0.01$; (b) $V_a = 10$.

precision. The integration involved in equations (14) has been accomplished numerically by the IMSL routines DQDAG and DTWODQ (using a globally adaptive scheme based on Gauss–Kronrod rules, with 7–15 points and a relative accuracy of 10^{-3} [8]). The results are plotted in some graphs; every graph contains several curves, each of them is made of 51 points. In spite of the double precision, the high accuracy and the numerous temperature values required, the CPU time for every figure is of the order of some hours on a very simple personal computer.

Figures 1–5 give a few examples of the several cases that have been run. As expected, the limiting results for V_a, $V_b \to 0$, and for $t \to \infty$, reproduce exactly those relevant to vanishing heat capacity ratios [5], and to steady-state operating conditions [1], respectively. Since the effects of heat capacity ratios seem to be the most important in the present time-dependent context, only their variations will be discussed in this paper, whereas the other physical parameters, i.e. E, R and NTU, will be kept constant and equal to unity. This implies in particuar $N_a = N_b = 2$ for the dimensionless lengths. The perturbation produced by the step entry reaches the exit section of the hot fluid at a time V_aN_a and then temperature increases, more slowly near the section $y = 0$ where the cold fluid enters, and approaches the steady-state profile. The unstepped fluid increases its temperature continuously, more rapidly near the section $x = 0$, where the hot fluid enters; the wave front propagates all over the x-axis, reaching the section $x = t/V_a$ at time t. Figure 1, where $V_a = V_b = 1$, shows T_a vs y at $x = N_a$, and analogously T_b vs x at $y = N_b$, for different times. This will be used as a reference case; notice the approach towards equilibrium when t increases. In Fig. 2 the same temperature profiles are plotted in the limiting case $V_a = V_b = 0$; now the infinite propagation speed of disturbances makes the approach to equilibrium faster and smoother. A comparison can be done with the step response dealt with in ref. [5]; the numerical values related in Fig. 2 are coincident with those presented in Figs. 1 and 2 of ref. [5], for $NTU = 1$. The opposite effect of a very slow propagation speed can be seen in Fig. 3, which is arranged like the previous ones, but with $V_a = V_b = 100$. Here the final steady state is approached very slowly (roughly speaking, there is a factor of 100 with respect to Fig. 1), and in a quite non-uniform way along the considered sections. In Fig. 4 all parameters are the same as in Fig. 1, except V_b which is taken equal to either 0.01 or 10. Only the propagation speed along the y-axis has been changed. This can be seen by comparison of the T_a profiles to the one of Fig. 1(a); when variations travel faster in the y-direction, T_a increases at about the same rate for y close to 0 as for y close to N_b, whilst in the opposite case the tail at large y follows with considerable delay the increase at $y = 0$. Figure 5 shows finally the temperature T_b with either $V_a = 0.01$ or 10, the other parameters being the same as in Fig. 1, so that only the speed of propagation in the x-direction is different. With reference to Fig. 1(b), the comment is, *mutatis mutandis*, the same as for Fig. 4. Notice in particular the presence of well-defined wavefronts for the values of t shown in the case of Fig. 5(b).

The main contribution of this paper consists in making available the exact two-dimensional temperature profiles in the single-pass crossflow heat exchanger. As its implication, mean temperatures and performance can be easily estimated, giving the designer useful information about surface area, configuration, and working parameters. Another meaningful practical significance and application of the solution resides in the possibility of carrying out a very detailed stress analysis, mainly concerning either the differential thermal expansion along both x- and y-axes, or the related thermal stresses.

Acknowledgements—This work was financially supported by the Italian National Research Council (CNR), through its Committees and the G.N.F.M., and by the Italian Ministry of Public Education (MPI).

REFERENCES

1. B. S. Baclic and P. J. Heggs, On the search for new solutions of the single-pass crossflow heat exchanger problem, *Int. J. Heat Mass Transfer* **28**, 1965–1976 (1985).
2. H. Yamashita, R. Izumi and S. Yamaguchi, Analysis of the dynamic characteristics of crossflow heat exchangers with both fluids unmixed, *JSME Bull.* **21**, 479–485 (1978).
3. F. E. Romie, Transient response of gas-to-gas crossflow heat exchangers with neither gas mixed, *J. Heat Transfer* **105**, 563–570 (1983).
4. D. D. Gvozdenac, Analytical solutions of the transient response of gas-to-gas crossflow heat exchangers with both fluids unmixed, *J. Heat Transfer* **108**, 722–727 (1986).
5. G. Spiga and M. Spiga, Two-dimensional transient solutions for crossflow heat exchangers with neither gas mixed, *J. Heat Transfer* **109**, 281–286 (1987).
6. M. Spiga and G. Spiga, Transient temperature fields in crossflow heat exchangers with finite wall capacitance, *J. Heat Transfer* **110**, 49–53 (1988).
7. M. Abramowitz and I. A. Stegun, *Handbook of Mathematical Functions*. Dover, New York (1972).
8. IMSL, *Math/Library*, Vol. 2. Houston, Texas (1987).

REPONSE A UN ECHELON POUR UN ECHANGEUR THERMIQUE CROISE AVEC CAPACITANCE FINIE DE PAROI

Résumé—On étudie la réponse à un échelon pour un échangeur thermique croisé à une seule passe. Les distributions variables et bidimensionnelles de température de la paroi et des fluides non mélangés sont déterminées analytiquement en considérant une capacité thermique finie de la paroi (c'est-à-dire une vitesse finie de propagation des perturbations). Les solutions sont déduites des équations de bilan local d'énergie à l'aide des fonctions de Green et d'une transformation de Laplace. Les températures adimensionnelles sont présentées en fonction des paramètres (nombre d'unités de transfert, rapport des capacités, rapport des résistances thermiques). En supposant des conditions initiales constantes et une température d'entrée du fluide chaud soumise à un accroissement brusque en échelon, le champ de température variable est calculé avec un temps de calcul extrêmement faible; les résultats sont donnés pour un large domaine des paramètres actifs.

SPRUNGANTWORT EINES KREUZSTROM-WÄRMEÜBERTRAGERS MIT ENDLICHER WÄRMEKAPAZITÄT DER WANDUNGEN

Zusammenfassung—Die Sprungantwort eines eingängigen Kreuzstrom-Wärmeübertragers wird untersucht. Die zweidimensionale instationäre Temperaturverteilung in der Wand und in beiden Fluidströmen, in denen keine Vermischung zugelassen wird, werden analytisch bestimmt. Dies geschieht unter Berücksichtigung der Wärmekapazität der Wand, was einer endlichen Ausbreitungsgeschwindigkeit von Störungen entspricht. Die Lösungen werden mit Hilfe von örtlichen Energiebilanzen, der Anwendung Green'scher Funktionen sowie einer dreifachen Laplace-Transformation abgeleitet. Die dimensionslose Temperaturverteilung wird als Funktion der maßgeblichen Parameter dargestellt: NTU, Verhältnis der Wärmekapazitätsströme, Verhältnis der Wärmeübergangswiderstände. Unter der Annahme einheitlicher Anfangsbedingungen und einer sprunghaften Änderung der Eintrittstemperatur des heißen Stromes wird das instationäre Temperaturfeld mit sehr geringer Rechenzeit bestimmt. Für einen weiten Bereich der Parameter werden Ergebnisse vorgestellt.

СТУПЕНЧАТАЯ ХАРАКТЕРИСТИКА ПЕРЕКРЕСТНОГО ТЕПЛООБМЕННИКА С КОНЕЧНОЙ ТЕПЛОЕМКОСТЬЮ СТЕНКИ

Аннотация—Исследуется ступенчатая характеристика одноходового перекрестного теплообменника. Двумерные распределения неустановившейся температуры в стенке внутри теплообменника и в обоих несмешанных жидкостях исследуются аналитически с учетом конечной теплоемкости стенки (т.е. конечной скорости распространения возмущений). Уравнения баланса локальной энергии решены с помощью функций Грина и трехкратного преобразования Лапласа. Безразмерные температуры выражены через определяющие параметры (число единиц переноса, отношение емкостей, отношение теплопереноса к сопротивлению). В предположении постоянства начальных условий и скачкообразного роста температуры нагретой жидкости на входе в предельно короткое время рассчитано распределение неустановившейся температуры. Результаты представлены в виде графика для широкого диапазона определяющих параметров.